Heliyon 10 (2024) e34677

Contents lists available at ScienceDirect

Heliyon

journal homepage: www.cell.com/heliyon

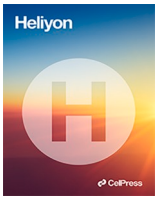

Research article

Gold-antibody-aptamer complexed electrochemical sensing surface for septic arthritis biomarker determination

Bin Yang [a,b], Faming Tian [c], Huilin Yu [a,b,*]

[a] Department of Orthopaedic Centre, Qilu Hospital (Qingdao), Cheeloo College of Medicine, Shandong University, 758 Hefei Road, Qingdao, 266000, Shandong, China
[b] Qingdao Medical Engineering Interdisciplinary Key Laboratory, Qilu Hospital (Qingdao), Shandong University, 758 Hefei Road, Qingdao, 266000, Shandong, China
[c] School of Public Health, North China University of Science and Technology, 21 Bohai Road, Caofeidian Xincheng, Tangshan, 063210, Hebei, China

ARTICLE INFO

Keywords:
Septic arthritis
Interdigitated electrode
Procalcitonin
Aptamer
Antibody

ABSTRACT

Septic arthritis (SA) is more severe in patients with rheumatoid arthritis, joint surgical issues, or a weakened immune system. Timely diagnosis of SA is crucial for effective treatment. Traditional diagnostic methods such as ELISA, white blood cell counting, blood culture, qPCR, and imaging techniques are often less accurate and time-consuming. Researchers are focusing on developing highly sensitive biosensors for SA using blood-based biomarkers. Procalcitonin is a protein and a well-established biomarker for SA. This research focuses on developing a procalcitonin interdigitated electrode (IDE) biosensor using a probe made of an aptamer and antibody-modified gold nanoparticle (AuNP) complex. The probe was attached to the IDE through an amine linker and then interacted with procalcitonin. AuNPs increased the attachment of the aptamer and antibody to the IDE, enabling the detection of procalcitonin at levels as low as 10 ng/mL, with a linear regression curve ranging from 10 to 100 ng/mL [$y = 4.0691x - 2.1887$; $R^2 = 0.9937$]. Furthermore, procalcitonin-spiked serum elevated the current level with increasing procalcitonin concentrations, while control performances did not enhance the current, indicating the selective and specific detection of procalcitonin. This AuNP-aptamer-antibody complexed biosensor effectively identifies procalcitonin at low levels and aids in the diagnosis of SA.

1. Introduction

Septic arthritis (SA) represents an infection and inflammation in a joint caused by different microorganisms such as fungi, bacteria, and viruses. In most cases, bacteria are primarily responsible for SA infections [1]. SA generally affects the large joints in the body, such as the hip and knee, and it rarely affects multiple joints. SA can be caused by bacteria that pass through the bloodstream from other parts of the body, by an open wound, or during surgery [2]. *Streptococcus* and *Staphylococcus* are the common bacteria that cause SA [3]. These bacteria enter the bloodstream, infect the joint, and cause pain and inflammation. Additionally, viruses that cause hepatitis, HIV, mumps, and adenovirus can also be responsible for SA infections. People with weakened immune systems, and those affected by diabetes, rheumatoid arthritis, and cancer, are at higher risk of developing SA [4]. Currently, antibody-based enzyme-linked

* Corresponding author. Department of Orthopaedic Centre, Qilu Hospital (Qingdao), Cheeloo College of Medicine, Shandong University, 758 Hefei Road, Qingdao, 266000, Shandong, China.
E-mail address: yhl370101@outlook.com (H. Yu).

https://doi.org/10.1016/j.heliyon.2024.e34677
Received 3 June 2024; Received in revised form 7 July 2024; Accepted 15 July 2024
Available online 22 July 2024

immunosorbent assay (ELISA) is the common technique used to identify SA. Other supporting diagnostic techniques include quantitative polymerase chain reaction (qPCR), white blood cell counting, and imaging. However, these methods are often less sensitive, costly, and time-consuming. Quantifying blood-based biological markers can help identify diseases at their early stages. Various biomarkers have been identified by researchers for diagnosing a wide range of diseases [5–12]. Procalcitonin is a protein that has been proven to be a suitable biomarker for SA. Quantifying the level of procalcitonin can help to overcome the limitations of conventional diagnostic methods for SA. This research focuses on developing an aptamer and antibody-based diagnostic method using an interdigitated electrode (IDE) to quantify the procalcitonin levels.

Aptamer is a DNA or RNA oligonucleotide selected from a randomized pool of molecules by using a method called, 'Systematic Evolution of Ligands by EXponential Enrichment (SELEX) [13]. Selected aptamers have attracted various fields and implemented in a wide range of applications [14]. Until now antibodies and nucleotides are the common molecules used as a probe to recognize the target element. Aptamers exhibit advantages as probe molecules in biosensors compared to the antibody [15,16]. Apart from that, aptamers are smaller in size, possible to modify easily, and cost-effective. In particular, aptamers are convenient and flexible in their structures, which led to create a novel biosensor that exhibited high selectivity and sensitivity [16–18]. The stem-loop structure of aptamers can make a versatile 3D structure, which helps to identify the closely related molecules [19]. Recently, the complexation of aptamers with other biomolecules and nanomaterials have enhanced the analytical performances [20]. In this research, on the surface of the gold nanoparticles (AuNP) aptamer and antibody were attached for a single target.

Nanomaterials have exclusive advantages with chemical, physical, and mechanical properties, are widely spread in various applications such as biosensors, preparation of insulating material, high energy density batteries, aerospace components, and long-lasting medical implants [21–24]. In particular, nanomaterials are well-established in the field of medicine, which includes tissue engineering, biosensors, drug delivery, and therapeutics [25–28]. Among other metals, gold is the most popular and used metal in the biomedical field due to its excellent biocompatibility, and easy surface modification [29,30]. In the current research, using the surface of AuNP, aptamer and antibody were attached through the chemical modification and immobilized on interdigitated electrode (IDE) to identify the procalcitonin.

Biosensor is a device, which can measure the chemical and biological reactions by generating signals through the transducer upon interactions of biomolecules. The signal output could help to identify various diseases and their conditions [31,32]. IDE is an established transducer, widely utilized in various analytical and technological applications due to its easier fabrication, higher-sensitivity and cheaper. In addition, suitable surface functionalization with various chemical and physical processes made easier to capture the molecules on the IDE. Various targets are identified on IDE for diagnosing different diseases such as cancer, diabetes, viral infection, and bacterial infection. Due to its micro-scale set-up, IDE needs only a lower volume of samples and can easily be carried out in rural places for diagnosing diseases. In this research, the IDE surface was converted into amine by modifying with 3-Aminopropyltriethoxysilane (APTES) followed by aptamer-antibody-modified AuNP conjugation. A higher number of probe attachments was expected through the nanoparticle-mediated surface functionalization, which enhances the analytical performance and lower the detection limit of procalcitonin.

2. Materials and methods

2.1. Reagents and biomolecules

(3-Aminopropyl)triethoxysilane (APTES), Phosphate buffered saline (PBS) stock, gold nanoparticle (AuNP), 16-mercaptohexadecanoic acid (16-MDA), Procalcitonin, anti-procalcitonin antibody, PEG-COOH, and human serum were bought from Sigma-Aldrich (USA). Thiol-ended specific aptamer sequence (5'–SH–CCGCGGCAGTTCCGTAATGTTAATGCCTATACTTGAGCTG-3′) and complementary aptamer sequence (5′–SH–GGCGCCGTCAAGGCATTACAATTACGGATATGAACTCGAC-3′) were commercially synthesized and received from a local supplier [33]. Interdigitated electrode (IDE) sensor was fabricated as described earlier and verified under High-power microscope [34,35]. The design of IDE was created with AutoCAD software and had the following dimensions: 11000 μm in length, 4500 μm in width, two 1250 μm square probing sites, and 18 pairs of 5 μm thick gap and finger areas. The system has been operated by a power supply from 0 to 2 V using an ammeter on a dual probe station. The intervals of 0.1 V were maintained with the above range.

2.2. Antibody attachment on AuNP

Aptamer and antibody on AuNP were prepared through chemical interaction. At first antibody (50 nM) was attached to the surface of AuNP and immobilized on IDE. After that aptamer was filled on the gap between antibody immobilized surface. For the process of antibody attachment on AuNP, as received AuNP was mixed with 16-MDA and kept for 30 min. After that, the bound 16-MDA-AuNP complex was recovered by centrifugation. Further, the surface of this complex was activated and stabilized by EDS and NHS followed by anti-procalcitonin antibodies were added and waited 1 h. The AuNP-antibody conjugation was recovered by centrifugation at 10,000×*g*, for 5 min. Similarly, other antibody concentrations, 100, 200, 400, and 800 nM on AuNP were prepared.

2.3. Optimization of antibody attachment on AuNP

Attachment of antibody-AuNP complex on IDE was optimized through the changes in current-volt on a prob-station to the IDE surface. The following steps were involved in this process; (i) IDE was treated with KOH for 5 min and rinsed with distilled water; (ii)

APTES (1 % diluted in 30 % EtOH) was added to IDE and rested overnight and the next day rinsed the IDE with diluted EtOH; (iii) Various concentrations of AuNP-antibody (50, 100, 200, 400, and 800 nM) conjugation were added and rested for 1 h. After 1 h, the surface was washed with 10 mM PBS (pH 7.4). Current changes were monitored for each preparation to identify the suitable concentration of AuNP-antibody conjugation.

2.4. Optimization of aptamer attachment on AuNP

Aptamer attachment on AuNP-antibody conjugated surface was optimized through the changes in current-volt on the IDE sensor. The following steps are involved in this process. (i) IDE was treated by KOH for 5 min and rinsed with distilled water; (ii) APTES (1 % diluted in 30 % EtOH) was added to IDE and rested overnight and the next day rinsed the IDE surface with diluted EtOH; (iii) Optimized concentration of AuNP-antibody was added and rested for 1 h. After 1 h surface was washed with PBS. (iv) Different concentrations of thiol-ended procalcitonin aptamer were added and rested for 30 min and washed the surface by PBS. Current changes were monitored for each aptamer concentration to identify the suitable conjugation of AuNP-antibody-aptamer conjugation.

2.5. Detection of procalcitonin by AuNP-antibody-aptamer

Procalcitonin was detected by the optimized AuNP-antibody-aptamer conjugation. The following steps are involved in this process. (i) IDE was treated by KOH for 5 min and rinsed with distilled water; (ii) APTES (1 % diluted in 30 % EtOH) was placed on IDE and rested overnight and the next day rinsed the IDE with diluted EtOH; (iii) Optimized complex level of AuNP-antibody was added and rested for 1 h. After 1 h surface was washed with PBS. (iv) Thiol-ended procalcitonin aptamer was added and rested for 30 min and washed the surface with PBS. (v) Different concentrations of procalcitonin were added on IDE and rested for 30 min. After that the surface was washed with PBS and the current changes were monitored for each procalcitonin concentration to identify the simultaneous interaction of procalcitonin with aptamer and antibody.

2.6. Sensitive and selective detection of procalcitonin

Selective detection of procalcitonin was assessed by experimenting with procalcitonin-spiked human serum. Procalcitonin (10–100 ng/mL) was diluted in human serum and placed on probe immobilized IDE. The current-volt measurement was recorded for each dilution with procalcitonin interaction. Specific procalcitonin detection was assessed by conducting an experiment with complementary aptamer; non-immune antibody; and control proteins (CTx-II, C reactive protein (CRP), Transforming growth factor alpha (TGF-α), and MCP-1). These are used instead of aptamer, antibody, and procalcitonin. The current-volt measurement was recorded for and compared with the specific detection of procalcitonin. Unless otherwise stated the measurements were performed at room temperature on a wet-surface and with thorough washings between each step using 10 reaction volume of 10 mM PBS (pH 7.4).

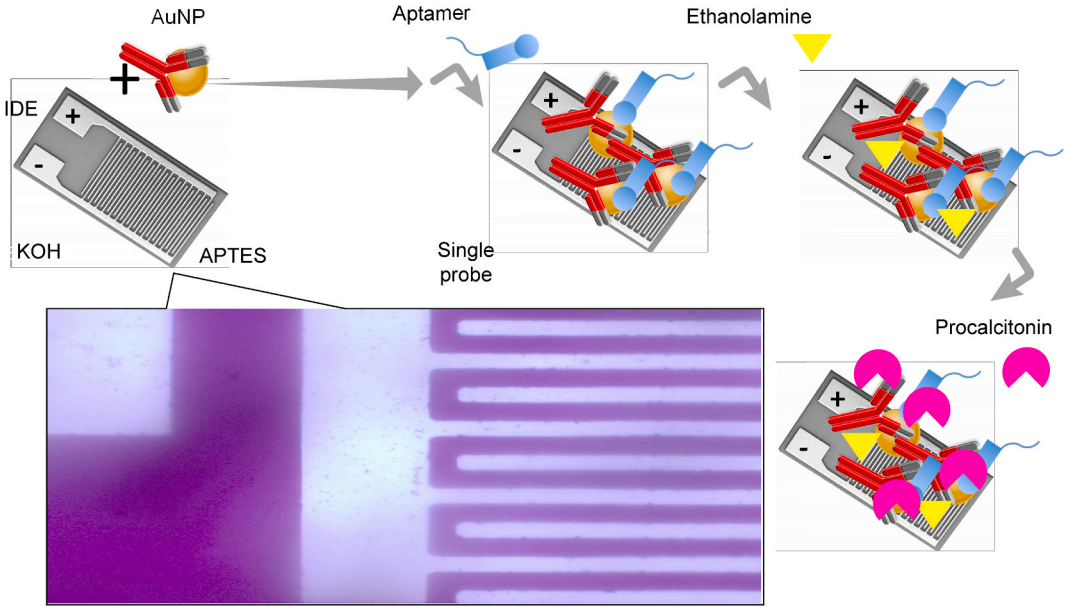

Fig. 1. Schematic illustration for procalcitonin biosensor. IDE was treated with KOH and then converted the surface into amine by APETS functionalization. Further, a probe molecule (AuNP-antibody-aptamer conjugation) was introduced to the electrode surface and then identified by procalcitonin. High-power microscope image on the IDE is displayed.

3. Results and discussion

Septic arthritis (SA) is a serious joint infection that is extremely painful and can affect people of any age. It needs to be treated immediately as an emergency. Diagnosing SA with higher sensitivity is essential to provide suitable treatment for affected individuals. Researchers are working towards developing a highly sensitive SA biosensor. Fig. 1 shows a schematic illustration of procalcitonin biosensors for diagnosing SA on an integrated electrode sensor (IDE). As shown in the figure, the IDE was treated with KOH and then converted to an amine surface by APTES treatment. Subsequently, a probe molecule (AuNP-antibody-aptamer conjugation) was added to the surface. This attachment occurred through the interaction of APTES with AuNP and the antibody. APTES can bind with the AuNP through electrostatic interaction, and it can bind with the antibody through the amine (with APTES) and the COOH in the antibody. Due to these two interactions, a higher number of probes were anchored to the IDE, lowering the detection limit of procalcitonin. IDE has a flat surface with a dual electrodes and in the presence of AuNP on the sensing surfaces, the surface area has been increased. The enhanced surface area is able to capture higher numbers of probes (aptamer and antibody).

A major prerequisite for the useful application of sensors is the detection of a specific target without compromising sensitivity. A variety of strategies have been proposed to properly determine the orientation of immobilized biomolecules in the development of higher sensitivity detection systems [36,37]. Herein, a dual-probe with antibody and aptamer on AuNP was prepared to detect SA biomarker of procalcitonin. Biomolecule-conjugated nanomaterials provide a higher number of probe attachments and a proper, stable orientation of biomolecules on the sensing surface. AuNP conjugated probe improves the aptamer and antibody attachment on IDE and interacts a higher number of procalcitonin.

3.1. AuNP-anti-procalcitonin antibody attachment on IDE

AuNP-anti-procalcitonin antibody was attached to IDE to identify the procalcitonin. To find a suitable concentration of antibody, different concentrations of antibody were tested on APTES-modified surface. Fig. 2a shows the current-volt measurement of antibody (50–800 nM) attachment on APTES. KOH-treated IDE shows the current level as 5.68E-08 A, after the surface was converted into amine by APTES, the current level was increased to 4.83 E−07 A. After that 50 nM of anti-procalcitonin antibody was introduced into the surface, and the current was increased to 2.13 E−06 A. This current change confirms the binding of the antibody on the APTES-modified surface. Further, increasing the concentration of antibodies to 100, 200, 40, and 800 nM, the current response increased gradually to 3.91 E−06 A, 1.19 E−05 A, 1.35 E−05 A, and 1.4 E−05 A, respectively. Current range was increased by increasing the antibody concentrations and the current level was saturated from 200 nM (Fig. 2b). It represents 200 nM of antibody is enough to occupy the complete APTES surface on IDE. Thus, 200 nM of antibody was used to detect procalcitonin.

3.2. AuNP-antibody-aptamer attachment on IDE

AuNP-antibody-aptamer was attached on IDE to identify the procalcitonin. The aptamer can attach to the gaps among antibodies on AuNP. Since an antibody has a larger size, it creates a gap among them. In general, these gaps are filled with blocking agents or by other molecule. In this study, filled the gap among antibodies with the anti-procalcitonin aptamer. Since aptamers are smaller in size and easily attached to AuNP through the thiol linker, they can fill in the gap among antibodies. Aptamer sequence was modified at the 5' end by thiol (–SH–) group and it has high affinity to the Au surface. So that, both antibody and aptamer can attach to the single AuNP, and it can interact a higher number of procalcitonin and enhance the analytical performance. To find an optimized aptamer level, concentrations from 50 to 800 nM were added on Au-antibody immobilized IDE surface. Fig. 3a shows the graph for the current-volt with aptamer attachment on AuNP. As shown in figure, 50 nM aptamer shows the increment in current response at 1.59 E−05 A. Further, increasing the concentrations of aptamer to 100, 200, 400, and 800 nM, the current responses were increased gradually to 2.10 E−05 A, 2.89 E−05 A, 3.26 E−05 A, and 3.44 E−05 A, respectively. Current range was increased by increasing the aptamer

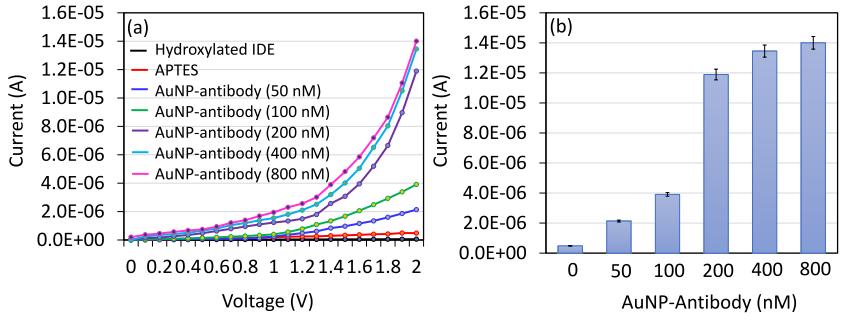

Fig. 2. AuNP-anti-procalcitonin antibody attachment on IDE. (a) Graph of current-volt with AuNP-antibody (50–800 nM) attachment on APTES modified IDE surface. A visible current increment was noticed for each antibody immobilization. (b) Current responses for different antibody concentrations on IDE. The current levels were increased by enhancing the antibody concentrations and the saturation was from 200 nM. Error values indicate the average of three independent experiments.

concentration and the current level as saturated from 200 nM (Fig. 3b). This indicated that 200 nM of aptamer is fair enough to fill the gap among antibodies on the surface. This AuNP-antibody-aptamer-modified electrode was utilized to quantify the level of procalcitonin.

3.3. Quantification of procalcitonin

Procalcitonin was quantified by its aptamer and antibody, for this, procalcitonin concentrations from 10 to 100 ng/mL were diluted and dropped interpedently on probe modified electrode. Fig. 4a shows the graph with the current-volt by procalcitonin interaction with its aptamer and antibody. Upon adding 10 ng/mL of procalcitonin, the current response was increased to 3.44 E−05 A, which confirms the interaction of procalcitonin. Further, with increasing the concentrations of procalcitonin to 20, 40, 60, 80, and 100 ng/mL, the current responses were increased gradually to 5.55 E−06 A, 9.21 E−05 A, 1.33 E−04 A, 1.70 E−04 A, 2.27 E−04 A, and 2.52 E−04 A, respectively (Fig. 4). The current levels were enhanced by increasing the procalcitonin concentrations. The current differences were plotted on a linear regression line and the limit of detection of procalcitonin was determined to be 10 ng/mL at the R^2 value of 0.9937 (Fig. 5a). This was achieved through the higher probe attachment by using AuNP and also the aptamer and antibody were immobilized on the single AuNP, which improved the interaction of procalcitonin on probe-immobilized IDE surface and enhanced the current responses.

3.4. Sensitive and selective identification of procalcitonin

Selective identification of procalcitonin was assessed though procalcitonin-spiked serum. Procalcitonin-spiked serum was added on the probe immobilized electrode surface and the current responses were recorded. As shown in Fig. 5b, the current level was increased by increasing the procalcitonin-spiked serum without any interference. This result confirms AuNP-antibody-aptamer-based detection system is capable of identifying procalcitonin in the serum or blood or actual patient sample, enabling to detection at the early stage of SA. Since human serum contains various biomolecules, increasing current responses indicating the selective detection of procalcitonin. Similarly, specific detection of procalcitonin was assessed through the control performances with complementary aptamer, non-immune antibody, and control proteins (CTx-II, CRP, TGF-α, and MCP-1). The control proteins are commonly presence in the patients with septic arthritis, which are abundance along with procalcitonin. As shown in Fig. 6, there is no notable difference in the current response with control proteins was recorded, indicating the specific detection of procalcitonin.

4. Conclusion

Septic arthritis (SA) is a serious acute atraumatic infection that must be promptly diagnosed and addressed. Risk factors for SA include old age, rheumatoid arthritis, diabetes, and recent joint surgery. Delaying the diagnosis of SA can lead to permanent morbidity and mortality. In this research, a highly sensitive procalcitonin biosensor was developed using an interdigitated electrode sensor. Antibody and aptamer-modified gold nanoparticles were used as the probe and immobilized on the electrode surface through amine modification. This probe-modified electrode surface interacts with a higher number of procalcitonin molecules, lowering the limit of detection to 10 ng/mL with an R^2 value of 0.9937. Furthermore, procalcitonin-spiked serum increases the current responses as procalcitonin concentrations increase, confirming the selective identification of procalcitonin. Additionally, control performances did not elevate the current level, indicating the specific detection of procalcitonin. This procalcitonin biosensor aids in diagnosing SA and associated conditions and can potentially be adapted for other biomarkers related to SA. The generated sensing platform in this study is a common and well-suited for other clinical and non-clinical markers. Even though, this sensing system improves the performance, the selection of probe (aptamer or antibody) and target with a high interaction is critical and mandatory.

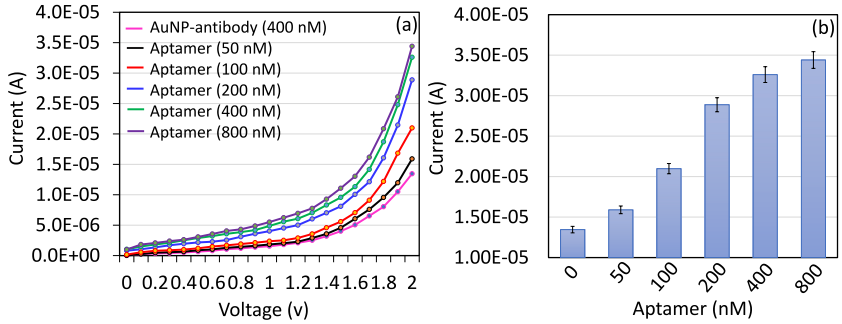

Fig. 3. AuNP-antibody-aptamer attachment. (a) Graph for current-volt with aptamer (50–800 nM) attachment on AuNP. A visible current increment was noticed for each aptamer immobilization. (b) Current response for different aptamer concentrations on AuNP. The current levels were increased by elevating the aptamer levels and the saturation was from 200 nM. Error values indicate the average of three independent experiments.

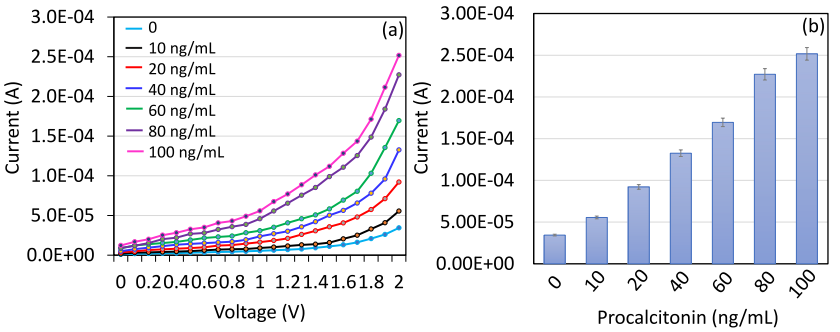

Fig. 4. (a) Detection of procalcitonin. (a) Graph for current-volt with procalcitonin interaction on IDE through aptamer and antibody. A clear increment of current was noticed by increasing the procalcitonin concentrations. (b) The current level at different concentrations of procalcitonin interaction on IDE. The current levels were increased by enhancing the concentrations of procalcitonin. Error values indicate the average of three independent experiments.

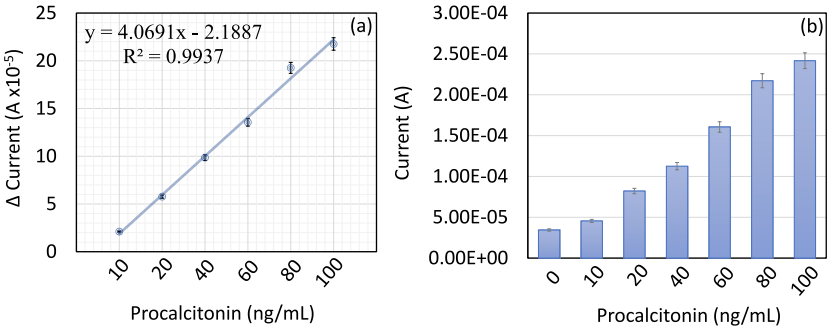

Fig. 5. (a) Limit of procalcitonin detection. (a) The current difference for each procalcitonin concentration was plotted on a linear regression line and the limit of procalcitonin detection was at 10 ng/mL with an R^2 value of 0.9937. (b) Selective identification of procalcitonin. Current levels were increased by increasing the procalcitonin-spiked serum without any interference, indicating the selective detection of procalcitonin. Error values indicate the average of three independent experiments.

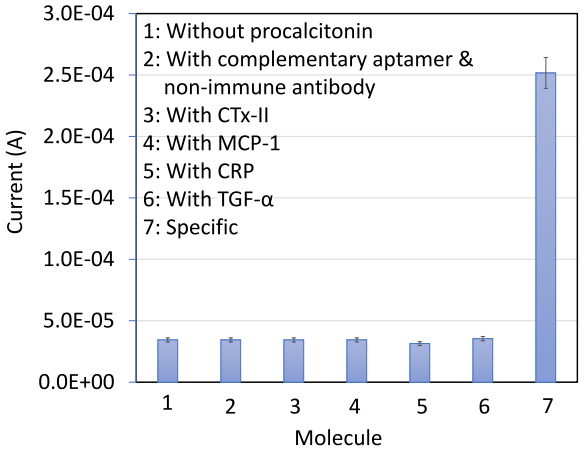

Fig. 6. Specific detection of procalcitonin. It was assessed through experiments with complementary aptamer, non-immune antibody, and control proteins. There is no notable difference in current changes recorded, indicating the specific detection of procalcitonin. Error values indicate the average of three independent experiments.

CRediT authorship contribution statement

Bin Yang: Writing – review & editing, Writing – original draft, Investigation, Formal analysis, Data curation. **Faming Tian:** Writing – review & editing, Validation, Software, Formal analysis. **Huilin Yu:** Writing – review & editing, Validation, Supervision, Resources, Project administration, Methodology, Funding acquisition, Conceptualization.

Declaration of competing interest

The authors declare that they have no known competing financial interests or personal relationships that could have appeared to influence the work reported in this paper.

References

[1] C.M. Donders, A.J. Spaans, H. van Wering, C.J.A. van Bergen, Developments in diagnosis and treatment of paediatric septic arthritis, World J. Orthoped. 13 (2022), https://doi.org/10.5312/wjo.v13.i2.122.

[2] J. Wang, L. Wang, Novel therapeutic interventions towards improved management of septic arthritis, BMC Muscoskel. Disord. 22 (2021), https://doi.org/10.1186/s12891-021-04383-6.

[3] P. Tzanis, K. Klavdianou, A. Lazarini, E. Theotikos, A. Balanika, A. Fanouriakis, A. Elezoglou, Septic arthritis complicating a gout flare: report of two cases and review of the literature, Mediterr J Rheumatol 33 (2022), https://doi.org/10.31138/MJR.33.1.75.

[4] M. Farrugia, B. Baron, The role of TNF-α in rheumatoid arthritis: a focus on regulatory T cells, J Clin Transl Res 2 (2016), https://doi.org/10.18053/jctres.02.201603.005.

[5] J. Song, H. Li, Y. Zhang, T. Wang, Y. Dong, H. Shui, J. Du, Effect of Dunaliella salina on myocardial ischemia-reperfusion injury through KEAP1/NRF2 pathway activation and JAK2/STAT3 pathway inhibition, Gene & Protein in Disease 2 (2023) 387, https://doi.org/10.36922/gpd.387.

[6] Y.-L. Ge, P.-Z. Wang, J.-H. Yan, W. Li, J.-R. Zhang, H. Jin, Y.-P. Yang, F. Wang, D. Li, J. Chen, K. Li, C.-J. Mao, C.-F. Liu, Associations of common variants in TAAR5, OR6C70, and GBA with hyposmia in Han Chinese individuals with Parkinson's disease, Advanced Neurology 1 (2022) 1–6, https://doi.org/10.36922/an.v1i2.71.

[7] H. Chen, N. Du, L. Wang, L. Yang, A higher risk for melanoma in patients with Parkinson's disease: based on the results from National Health and Nutrition Examination Survey 2001 – 2004, Journal of Clinical and Basic Psychosomatics 1 (2023) 571, https://doi.org/10.36922/jcbp.0571.

[8] X. Wang, Y. Xu, S. Zhang, Y. Qu, D. Wang, X. An, L. Zeng, W. Xu, Y. Wu, H. Chen, Q. Wang, J. Ai, MicroRNA-195 rescues the impaired MS-dCA1 neural circuit and spatial memory in rats with chronic cerebral hypoperfusion, Advanced Neurology 1 (2022) 116, https://doi.org/10.36922/an.v1i2.116.

[9] F.A. Khan, B. Nsengimana, N.H. Khan, J. Huang, H. Guo, U. Ayub Awan, W. Zhang, W. Wei, S. Ji, Differential Expression Profiles of circRNAs in Cancers: Future Clinical and Diagnostic Perspectives, Gene & Protein in Disease, 1, 2022, p. 138, https://doi.org/10.36922/gpd.v1i2.138.

[10] R. Shinde, I. Juwarwala, V. Modi, C.V. Chandarana, Utility of cardiac biomarkers and biosensors for diagnosis of acute myocardial infarction, Global Translational Medicine 2 (2023) 403, https://doi.org/10.36922/gtm.0403.

[11] Circulating plasma microRNA-126, -145 and -155 and their association with atherosclerotic plaque characteristics, J Clin Transl Res (2019), https://doi.org/10.18053/jctres.05.201902.002.

[12] Y. Chen, W. Zhou, Y. Gong, X. Ou, A N6-methyladenosine-related long noncoding RNA is a potential biomarker for predicting pancreatic cancer prognosis, Tumor Discovery 1 (2022) 165, https://doi.org/10.36922/td.v1i2.165.

[13] Y. Huang, L. Zhang, Z. Li, S.C.B. Gopinath, Y. Chen, Y. Xiao, Aptamer–17β-estradiol–antibody sandwich ELISA for determination of gynecological endocrine function, Biotechnol. Appl. Biochem. 68 (2021), https://doi.org/10.1002/bab.2008.

[14] Jian Luo, Subash C.B. Gopinath, Sreeramanan Subramaniam, Zaifeng Wu, Arthritis biosensing, Aptamer-antibody-mediated identification of biomarkers by ELISA, Process Biochem. 121 (2022) 396–402.

[15] T. Lakshmipriya, Y. Horiguchi, Y. Nagasaki, Co-immobilized poly(ethylene glycol)-block-polyamines promote sensitivity and restrict biofouling on gold sensor surface for detecting factor IX in human plasma, Analyst 139 (2014) 3977–3985, https://doi.org/10.1039/c4an00168k.

[16] T. Lakshmipriya, M. Fujimaki, S.C.B. Gopinath, K. Awazu, Generation of anti-influenza aptamers using the systematic evolution of ligands by exponential enrichment for sensing applications, Langmuir 29 (2013) 15107–15115, https://doi.org/10.1021/la4027283.

[17] L. Liu, S.C.B. Gopinath, Y.S. Wu, W. Zhao, Gold-enhanced current-volt dielectrode junction for biosensing with an aptamer-insulin-like growth factor-1-antibody sandwich pattern, Materials Express 12 (2022), https://doi.org/10.1166/mex.2022.2153.

[18] D. Lu, L. He, G. Zhang, A. Lv, R. Wang, X. Zhang, W. Tan, Aptamer-assembled nanomaterials for fluorescent sensing and imaging, Nanophotonics 6 (2016) 109–121, https://doi.org/10.1515/nanoph-2015-0145.

[19] Z. Zhang, Y. Zhu, X. Ma, H. Chai, P. Miao, Ultrasensitive electrochemical detection of VEGF based on split aptamers-controlled two-dimensional DNA assembly, Chem. Eng. J. 485 (2024), https://doi.org/10.1016/j.cej.2024.149912.

[20] X. Chen, Z. Guo, Y. Tang, Y. Shen, P. Miao, A highly sensitive gold nanoparticle-based electrochemical aptasensor for theophylline detection, Anal. Chim. Acta 999 (2018), https://doi.org/10.1016/j.aca.2017.10.039.

[21] M. Taguchi, A. Ptitsyn, E.S. McLamore, J.C. Claussen, Nanomaterial-mediated biosensors for monitoring glucose, J. Diabetes Sci. Technol. 8 (2014) 403–411, https://doi.org/10.1177/1932296814522799.

[22] W. Yu, Z. Xiao, X. Zhang, Y. Sun, P. Xue, S. Tan, Y. Wu, H. Zheng, Processing and characterization of crack-free 7075 aluminum alloys with elemental Zr modification by laser powder bed fusion, Materials Science in Additive Manufacturing 1 (2022) 4, https://doi.org/10.18063/msam.v1i1.4.

[23] C.T. Pan, K. Dutt, A. Kumar, R. Kumar, C.H. Chuang, Y.T. Lo, Z.H. Wen, C.S. Wang, S.W. Kuo, PVDF/AgNP/MXene composites-based near-field electrospun fiber with enhanced piezoelectric performance for self-powered wearable sensors, Int J Bioprint 9 (2022) 336–353, https://doi.org/10.18063/IJB.V9I1.647.

[24] M.S. Yusoff, S.C.B. Gopinath, M.N.A. Uda, T. Lakshmipriya, A.R. Wan Yaakub, P. Anbu, Conjugation of silver and gold nanoparticles for enhancing antimicrobial activity, INNOSC Theranostics and Pharmacological Sciences 4 (2022) 38–47, https://doi.org/10.36922/itps.v4i2.70.

[25] A. Kushwaha, L. Goswami, B.S. Kim, Nanomaterial-based therapy for wound healing, Nanomaterials 12 (2022) 618, https://doi.org/10.3390/nano12040618.

[26] P. Sarvari, P. Sarvari, Advances in nanoparticle-based drug delivery in cancer treatment, Global Translational Medicine 2 (2023) 394, https://doi.org/10.36922/gtm.0394.

[27] H. Jung Jo, M. Sung Kang, H. Jeong Jang, I. Selestin Raja, D. Lim, B. Kim, D.-W. Han, Advanced approaches with combination of 2D nanomaterials and 3D printing for exquisite neural tissue engineering Materials Science in, Addit. Manuf. 2 (2023) 1, https://doi.org/10.36922/msam.0620.

[28] M. Heidari Majd, Dual-targeting and specific delivery of tamoxifen to cancer cells by modified magnetic nanoparticles using hyaluronic acid and folic acid, Tumor Discovery 1 (2022) 1–9, https://doi.org/10.36922/td.v1i1.41.

[29] J.C. Liu, Z.Z. Lu, A.L. Chen, Gold nanoparticle-aptamer based colorimetric biosensing assays, Spectrosc. Spectr. Anal. 34 (2014) 2040–2046, https://doi.org/10.3964/j.issn.1000-0593(2014)08-2040-07.

[30] J. Lee, M. Morita, K. Takemura, E.Y. Park, A multi-functional gold/iron-oxide nanoparticle-CNT hybrid nanomaterial as virus DNA sensing platform, Biosens. Bioelectron. 102 (2018) 425–431, https://doi.org/10.1016/j.bios.2017.11.052.

[31] M. Iversen, M. Monisha, S. Agarwala, Flexible, wearable and fully-printed smart patch for pH and hydration sensing in wounds, Int J Bioprint 8 (2022) 41–49, https://doi.org/10.18063/IJB.V8I1.447.

[32] H. Geng, S.C.B. Gopinath, W. Niu, Highly sensitive hepatitis B virus identification by antibody-aptamer sandwich enzyme-linked immunosorbent assay, INNOSC Theranostics and Pharmacological Sciences 5 (2023) 7–14, https://doi.org/10.36922/itps.298.
[33] D.Y. Park, W.R. Shin, S.Y. Kim, Q.T. Nguyen, J.P. Lee, D.Y. Kim, J.Y. Ahn, Y.H. Kim, In silico molecular docking validation of procalcitonin-binding aptamer and sepsis diagnosis, Mol Cell Toxicol (2023), https://doi.org/10.1007/s13273-023-00384-9.
[34] A. Ghosh, S.C.B. Gopinath, S.M. Firdous, S. Ramanathan, Early detection of viral DNA in breast cancer using fingered aluminium interdigitated electrode modified by Streptavidin-biotin tetravalent complex, J. Indian Chem. Soc. 99 (2022), https://doi.org/10.1016/j.jics.2022.100604.
[35] B. Yao, Z. Li, S. Wang, S.C.B. Gopinath, P. Anbu, J. Shao, Osteoporosis biomarker 'c-terminal telopeptide' identification on carbon nanofiber-modified interdigitated electrode sensor, Appl. Phys. Mater. Sci. Process 128 (2022) 743, https://doi.org/10.1007/s00339-022-05823-3.
[36] T. Lakshmipriya, U. Hashim, S.C.B. Gopinath, N. Azizah, Microfluidic-based biosensor: signal enhancement by gold nanoparticle, Microsyst. Technol. 22 (2016) 2389–2395, https://doi.org/10.1007/s00542-016-3074-1.
[37] S.C.B. Gopinath, S. Ramanathan, M.N.M. Yasin, M.I. Shapiai, Z.H. Ismail, S. Subramaniam, Essential semiconductor films in micro-/nano-biosensors: current scenarios, J. Taiwan Inst. Chem. Eng. 127 (2021) 302–311, https://doi.org/10.1016/j.jtice.2021.07.036.